IMPACT RESPONSES AND FAILURE MECHANISMS OF AlMgB14 UNDER DYNAMIC LOADS

Yanyan Lu[1], Wenzhi Wang[1], Yushu Zhang[2], Zhenyi Zhang[3,*]

[1] School of Aeronautics, Northwestern Polytechnical University, Xi'an, Shaanxi, 710072, China

[2] Hangzhou Zhiyuan Research Institute, Hangzhou, Zhejiang, 310024, China

[3] Northwest Institute of Mechanical and Electrical Engineering, Xianyang, Shaanxi, 712099, China

Abstract

$AlMgB_{14}$ is a promising candidate for ballistic protection due to high hardness and low density, but its mechanical behaviours under dynamic loads remain unclear. In this study, the impact responses and failure mechanisms of $AlMgB_{14}$ under dynamic loading were systematically evaluated through experimental methods. The ultimate compressive strength of $AlMgB_{14}$ remained basically unchanged under the strain rate from 250 s^{-1} to 400 s^{-1}. The average residual depth of penetration of $AlMgB_{14}$ was 43.37 mm, which revealed a high mass efficiency. Target plate test showed that the typical failure mode of $AlMgB_{14}$ ceramic had radial and circumferential cracks around the bullet hole, which absorbed lots of impact energy of the projectile, leading to the lower bulge of the backing material. This study provides the ballistic performance evaluation on $AlMgB_{14}$ for the design of protective structures using this ultra-hard material.

Keywords: ballistic performance; $AlMgB_{14}$; mechanical behaviours

1. General Introduction

In modern warfare, the amalgamation of shrapnel and shockwaves poses a formidable challenge to the protective capabilities of conventional body armour systems. The typical body armour systems can be divided into soft and hard body armour[1]. The types of soft body armour are basically made of high-performance fibres with light weight and typical flexibility, such as aramid, and ultra-high molecular weight polyethylene (UHMWPE) fibers[2], [3], [4]. Soft armour is capable of protecting wearer against low to medium project velocities (up to 500 m/s)[5], which is widely used in personnel ballistic protective clothing for military and law enforcement application. On the other hand, hard body armour is designed to against higher projectile velocities (850 m/s or higher), which is mainly composed of ceramic, metal and composite plates[6].

During ballistic impact, the high hardness and high compressive strength of ceramic materials contribute to deflect or destruct the projectile tip, and distribute the load over a large area of the backing[7], [8]. In general, alumina (Al_2O_3), silicon carbide (SiC) and boron carbide (B_4C) have been widely applied in armour design[9], [10]. Among them, B_4C is much lighter (2.5 g/cm^3)[11] and possesses higher hardness (25.5 GPa)[12], and thus is well-known for its ballistic resistance. The ceramics in hard armour system destroy the projectile tip due to their high strength and hardness, and absorb impact energy due to high fracture toughness[13]. The lightweight requirements of military equipment necessitate the development of new and more advanced ceramic materials. The aluminum magnesium boride $AlMgB_{14}$ is a very promising candidate for ballistic protection because of its high hardness and fracture toughness, and low density. $AlMgB_{14}$ has the similar density (2.59 g/cm^3) to B_4C[14], while it excels in higher hardness (25 to 35 GPa) and fracture toughness (5.59 ± 0.42 $MPa \cdot m^{1/2}$)[15], [16].

Most research on $AlMgB_{14}$ mainly focused on its synthesis, manufacture and structure[17], [18], [19], while the mechanical properties of $AlMgB_{14}$ have been reported only in a limited number of works. The coefficient of thermal expansion of $AlMgB_{14}$ was measured by dilatometry and by high temperature X-ray diffraction, which is close to that of Ti and steel[20]. The flexural strength and flexural modulus

of $AlMgB_{14}$-based ceramic materials from varying hot-pressing conditions were investigated[21]. However, the ballistic properties of $AlMgB_{14}$ have been rarely reported, which limits the further application of this material in body armour system. This paper systematically investigated the impact behaviours and failure mechanisms of $AlMgB_{14}$ under dynamic loads through a combination of experimental tests, providing crucial insights for the design and development of innovative protective structures using $AlMgB_{14}$ ceramic.

2. Experimental Methods

2.1 SHPB Test

To examine the mechanical properties of $AlMgB_{14}$ under dynamic loading, the split Hopkinson pressure bar (SHPB) test was conducted using cylindrical specimens. Before the test, the loading surfaces of the specimen were polished and lubricated to minimize the interfacial friction. The schematics of the SHPB test is shown in Fig. 1. A pair of tungsten alloy cushion block was placed between the incident bar and the projection bar. The strain rate taken in the SHPB test was between $250s^{-1}$ and $400s^{-1}$.

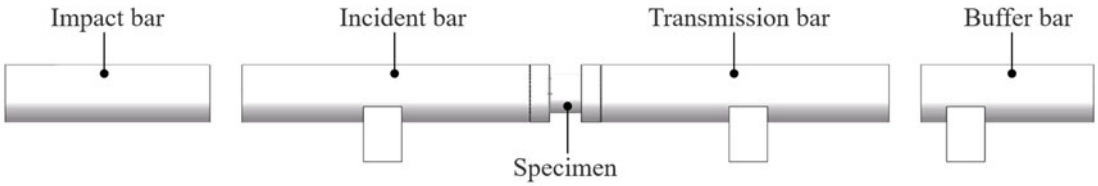

Fig. 1 Schematic split Hopkinson pressure bar

2.2 DOP Test

To evaluate the ballistic resistance of $AlMgB_{14}$, the depth of penetration (DOP) test was conducted. Fig. 2 shows a schematic of DOP test setup, which is mainly composed of a launch device and a combined target. The velocity of 12.7 mm projectile was 840 m/s. The test target is a $AlMgB_{14}$ ceramic plate with a thickness of 6 mm, and the backing material is a cylindrical ingot made of 2024 aluminum alloy with a radius of 80 mm and a height of 100 mm, which can be regarded as a semi-infinitely thick target plate in the test. Four $AlMgB_{14}$ tiles (AMB-1 to AMB-4) with 2024 aluminum alloy as the backing material were carried out for DOP tests. The DOP test of $AlMgB_{14}$ ceramics was carried out for four times. After the test, the $AlMgB_{14}$ ceramic plates were removed, and the depth of penetration in the 2024 aluminum alloy was measured.

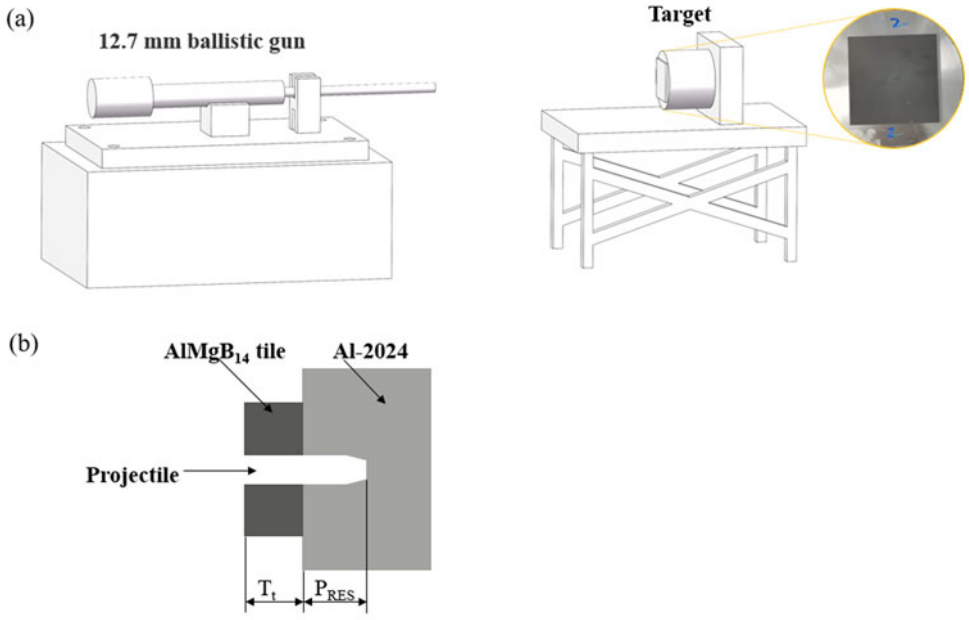

Fig.2 (a) Schematic of depth of penetration (DOP) test. (b) Target configuration in DOP test.

2.3 Target Plate Test

To evaluate the ballistic performance of $AlMgB_{14}$, the ballistic test of $AlMgB_{14}$ bonded with appropriate

backing materials was conducted. Due to the limitation of the preparation process, only the $AlMgB_{14}$ ceramic plates with the maximum size of 100 × 100 mm can be prepared. Therefore, multiple target tiles are spliced together to form a standard test target plate.

The process for the preparation of target plate is shown in Fig. 3(a). First, 6 pieces of 100 mm × 100 mm and 3 pieces of 50 mm × 100 mm $AlMgB_{14}$ ceramic tiles with a thickness of 7 mm were prepared. Then these $AlMgB_{14}$ tiles were glued together to form a whole ceramic plate of 300 mm × 250 mm. The second metallic plate was made of 1 mm TC4 with same length and width as the ceramic plate. The back plate was made of UHMWPE with a thickness of 10 mm and the same size as the TC4 metal plate. Epoxy resin glues were used to bond three layers together to form a laminated target plate (7 mm $AlMgB_{14}$+1 mm TC4+10 mm UHMWPE) with a surface density of 32.77 kg/m^2. The front and side views of the test target is shown in Fig. 3(a) and 3(b), and the experimental plate is shown in Fig. 3(c). The plate is numbered and divided into 8 targets (#1–#8). After the test is completed, the strike-face ceramic and the backing material are recycled, and the diameter of the hole in the strike-face material and the bulge deformation of the backing material are measured.

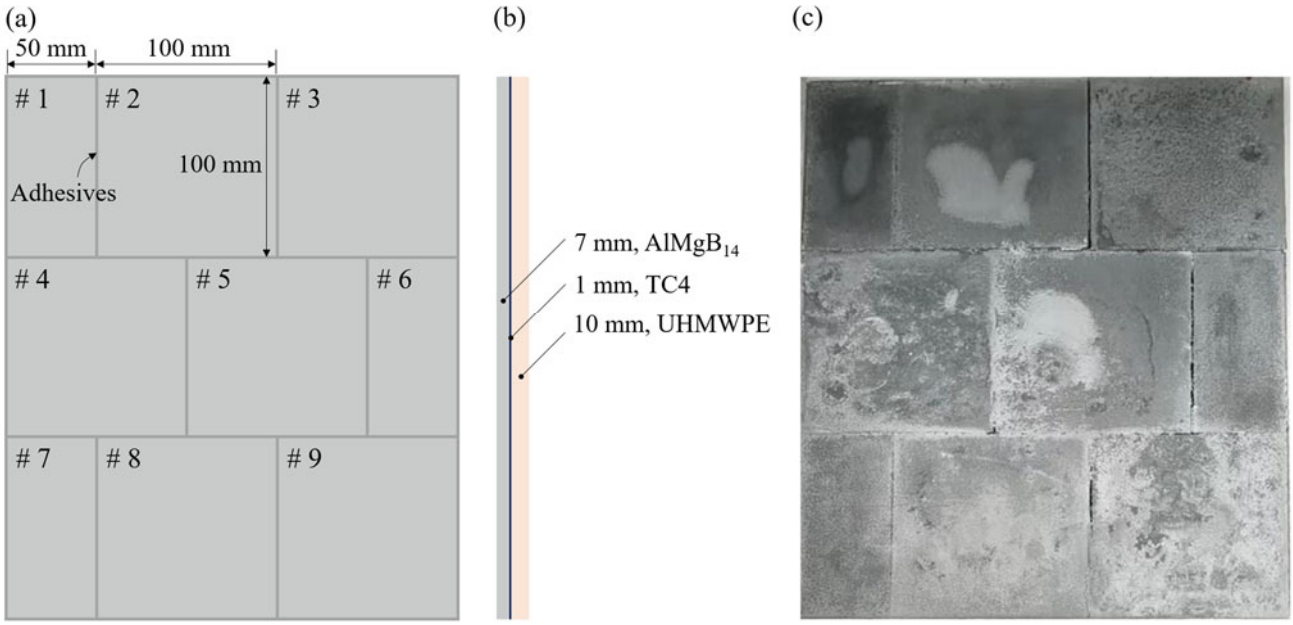

Fig. 3 Schematics of the (a) front view and (b) side view of the target plate. (c) Experimental target plate.

3. Results and Discussion

3.1 Dynamic Compressive Strength

Fig. 4 shows the compressive strength of $AlMgB_{14}$ at different strain rates. As the strain rate increased from 250 s^{-1} to 400 s^{-1}, the ultimate compressive strength remained basically unchanged. The result indicated that the dynamic compressive strength of $AlMgB_{14}$ ceramics was insensitive to strain rate at the range of 250 s^{-1}–400 s^{-1}.

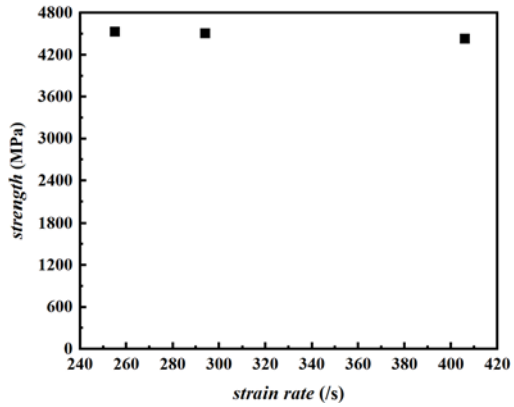

Fig.4 Compressive strength of $AlMgB_{14}$ at different strain rates

3.2 DOP Test Results

Fig. 5(a) shows the failure morphology of the 2024 aluminum alloy target in DOP test with $AlMgB_{14}$ tile, and Fig. 5(b) shows the failure morphology of reference 2024 aluminum alloy. Different from the flanging and tearing damage at the bullet hole in a reference semi-infinite 2024 aluminum alloy, the bullet hole in the combined target with $AlMgB_{14}$ tile and semi-infinite 2024 aluminum alloy was more rounded, and presented a funnel-shaped hole. This phenomenon can be attributed to the interaction between the projectile and $AlMgB_{14}$ ceramics during the penetration process. The $AlMgB_{14}$ ceramic, owing to its high hardness, exerts abrasive and blunting effects on the projectile. This interaction decreases the projectile's mass and velocity, subsequently enhancing the penetration resistance of the target plates. As a result, the final bullet hole is smooth and rounded.

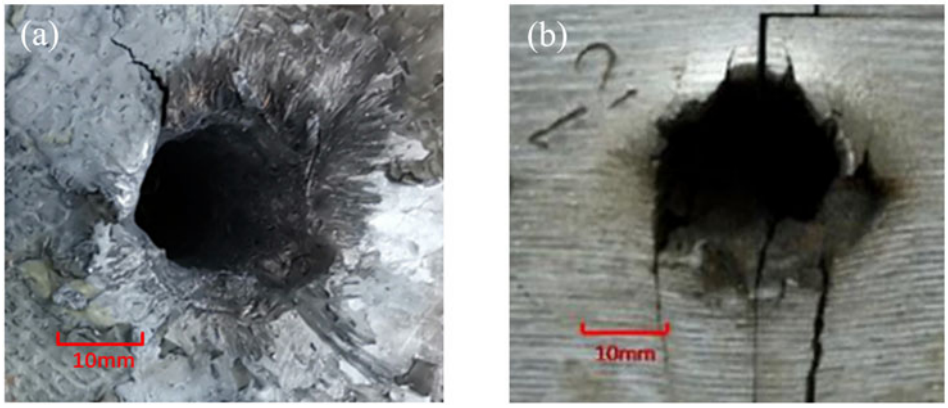

Fig.5 Failure morphology of (a) the 2024 aluminum alloy target in DOP test with $AlMgB_{14}$ tile[22] and (b) the reference 2024 aluminum alloy[23].

The experimental results of the DOP test of four $AlMgB_{14}$ ceramic tiles are shown in Table 1. The result shows that the average residual DOP of $AlMgB_{14}$ was 43.37 mm. Compared with the reference penetration of 70 mm in a semi-infinite 2024 aluminum alloy[23], the penetration depth in this study is 38.04% less than that of reference test. The $AlMgB_{14}$ ceramic plate with a thickness of 6 mm exhibits protective performance comparable to that of D95 ceramic plate with a thickness of 10 mm[24], and the density of $AlMgB_{14}$ ceramic is only 70% of that of D95 ceramic. It can be concluded that $AlMgB_{14}$ ceramics present significant advantages as a ballistic material, characterized by their low density, high hardness, and superior penetration resistance.

Table 1 Ballistic experimental results on $AlMgB_{14}$ tiles radially confined with 2024 aluminum alloy[22]

Experiment Nos.	Residual penetration (mm)	Average residual penetration (mm)
AMB-1	43.44	43.37
AMB-2	45.31	
AMB-3	43.69	
AMB-4	41.04	

The ballistic performance of ceramic can be evaluated by comparing the DOP of the projectile in a reference semi-infinite thick aluminum alloy (Al-2024) target plate to that of a combined target with ceramic armour tile and semi-infinite thick aluminum alloy (Al-2024). The ballistic performance of the ceramic is calculated in terms of the mass efficiency E_m as given in Equation (1)[25], [26]:

$$E_m = \frac{(P_{REF} - P_{RES})\,\rho_{REF}}{T_t\,\rho_t} \tag{1}$$

where P_{REF} is the baseline penetration of the 2024 aluminum alloy, and P_{RES} is the residual penetration depth of the combined target with ceramic armour tile and aluminum alloy (Al-2024). ρ_{REF} is the density of the reference 2024 aluminum alloy, and T_t and ρ_t are the thickness and density of the $AlMgB_{14}$ tile, respectively. The mass efficiency of $AlMgB_{14}$ at the projectile velocity of 840 m/s is 5. This result indicates that the $AlMgB_{14}$ is thinner and lighter than the equivalent reference material, and has superior performance.

3.3 Projectile Penetration Results of Target Plate

Projectile penetration experiments were carried out on eight $AlMgB_{14}$ ceramic tiles, of which two

projectiles penetrated the target plate and the remaining six were stuck in the target plate. Fig. 6 shows the broken shape of the target plate after projectile penetration test.

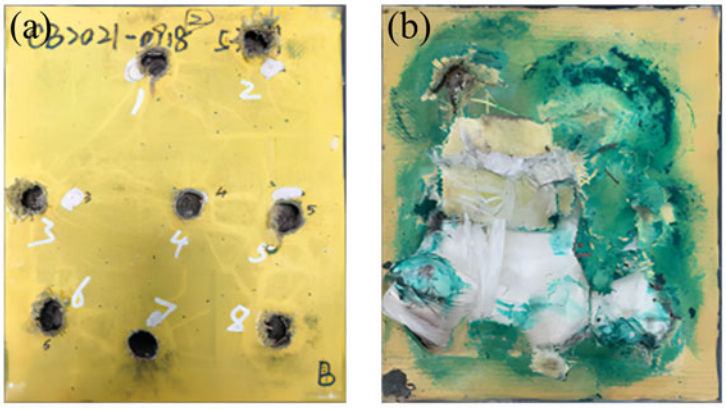

Fig. 6 Photograph of target plate after test: (a) front view and (b) back view.

The bulge deformation of each target is shown in Table 2, and Fig. 7 shows the broken morphology of the $AlMgB_{14}$ ceramic panels obtained by X-ray. The average diameter of bullet hole on $AlMgB_{14}$ ceramic was 26.71 mm, with a variation coefficient of 16.10%. The average bulge deformation of backing UHMWPE was 49.67 mm, with a variation coefficient of 23.97%. The diameter of bullet hole in $AlMgB_{14}$ ceramic is mainly affected by the physico-mechanical properties of the ceramic, such as Young's modulus, hardness, and resistance to brittle fracture, leading to a smaller dispersion in hole size. However, the projectile impacted the UHMWPE after destroyed by the ceramic, and thus the bulge deformation in the backing material is closely related to the energy absorption in the strike-face ceramic. Due to the large deviation of the shot position in $AlMgB_{14}$ tile and the different sizes of tiles, the energy absorption in each tile is different, which results in a higher difference in the bulge deformation of the backing material.

Table 2 Impact velocities of projectiles and corresponding deformations of the target plate.

Parameter	#1	#2	#3	#4	#5	#6	#7	#8
Impact velocity (m/s)	878	873	877	875	877	874	875	878
Diameter of bullet hole (mm)	30.9	22.8	28.1	28.8	33.8	22.5	23.9	22.9
Bulge deformation (mm)	40.4	61.5	37.3	Penetration	40.8	52.8	65.2	Penetration

The average bulge deformation is 49.67 mm, and largest deformation occurred at target #7. Because the impact position of target #7 located between $AlMgB_{14}$ tiles #7 and #8 (Fig.7 (a)), the cracks caused by the projectile in target #7 cannot extend to the surrounding tiles (Fig.7 (c)), which reduces the energy absorbed by ceramics and increases the deformation in UHMWPE to absorb redundant energy. As shown in Fig. 7(b), the typical failure situation of ceramic panel (target #3) had radial and circumferential cracks around the bullet hole, which is consistent with the ceramic failure phenomenon in previous studies[27], [28]. When the ceramics are impacted, there are radial cracks and circumferential cracks, and the inside of the ceramic will form a cone-shaped failure. It can be inferred that the $AlMgB_{14}$ ceramic can be used as protective materials to absorb impact energy of the projectile, and thus leads to the lowest bulge deformation in target #3.

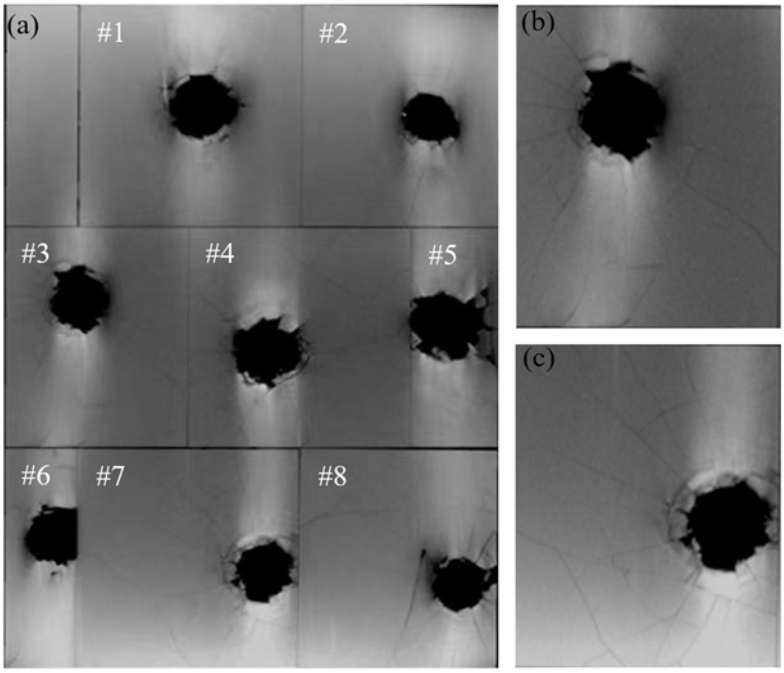

Fig. 7 Broken shapes of (a) the whole target plate and (b) #3 and (c) #7 ceramic panels obtained by X-ray.

4. Conclusion

The impact responses and failure mechanisms of $AlMgB_{14}$ under dynamic loads were studied through experimental methods. The major conclusions drawn from the findings of this study are summarized below:

(1) As the strain rate increased from 250 s^{-1} to 400 s^{-1}, the ultimate compressive strength of $AlMgB_{14}$ remained basically unchanged, which indicates that the strength of $AlMgB_{14}$ is insensitive to strain rate at this range.

(2) The average residual DOP of $AlMgB_{14}$ was 43.37 mm, which was 38.04% less than that of reference test and revealed a higher mass efficiency.

(3) The failure morphology of $AlMgB_{14}$ in target plate test showed radial cracks and circumferential cracks, which increased the absorption of impact energy and decreased the bulge deformation in backing material.

This study provides ballistic performance evaluation of the ultra-hard $AlMgB_{14}$ and demonstrates that $AlMgB_{14}$ has excellent ballistic impact resistance, which can give guidance on the design of protective structures using this material.

5. Contact Author Information

Zhenyi Zhang, Northwest Institute of Mechanical and Electrical Engineering, Xianyang, Shaanxi, 712099, China. E-mail: 814215950@qq.com.

6. Copyright Statement

References

[1] Mawkhlieng U., Majumdar A., and Laha A. A review of fibrous materials for soft body armour applications. RSC Advances, Vol. 10, No. 2, pp. 1066-1086, 2020.

[2] Yang Y. F., and Chen X. G. Determination of materials for hybrid design of 3D soft body armour panels. Applied Composite Materials, Vol. 25, pp. 861-875, 2018.

[3] Bajya M., Majumdar A., and Butola B. S. A review on current status and development possibilities of soft armour panel assembly. Journal of Materials Science, Vol. 58, No. 38, pp. 14997-15020, 2023.

[4] Bajya M., Majumdar A., Butola B. S., and Jasra R. V. Exploration of disentangled UHMWPE tape as a soft body armour material. Materials Chemistry and Physics, Vol. 295, pp. 127162, 2023.

[5] Naveen J., Jayakrishna K., Hameed Sultan M. T. B., and Amir S. M. M. Ballistic performance of natural fiber based soft and hard body armour-a mini review. Frontiers in Materials, Vol. 7, pp. 608139, 2020.

[6] Mawkhlieng U., and Majumdar A. Soft body armour. Textile Progress, Vol. 51, No. 2, pp. 139-224, 2019.

[7] Bracamonte L., Loutfy R., Yilmazcoban I. K., and Rajan S. D. Lightweight ballistic composites: Military and law-enforcement applications. 2nd edition, Woodhead Publishing Series in Composites Science and Engineering, Cambridge, 2016.

[8] Cegła M., Habaj W., Stępniak W., and Podgórzak, P. Hybrid ceramic-textile composite armour structures for a strengthened bullet-proof vest. Fibres and Textiles in Eastern Europe, Vol. 1, No. 109, pp. 85-88, 2015.

[9] Karabulut Ş., Gökmen U., and Cinici H. Study on the mechanical and drilling properties of AA7039 composites reinforced with Al_2O_3/B_4C/SiC particles. Composites Part B: Engineering, Vol. 93, pp. 43-55, 2016.

[10] Silveira P. H. P. M., Silva T. T., Ribeiro M. P., Jesus P. R. R., Santos Credmann P. C. R., and Gomes A. V. A brief review of alumina, silicon carbide and boron carbide ceramic materials for ballistic applications. Academia Letters, Vol. 3742, pp. 1-11, 2021.

[11] Domnich V., Reynaud S., Haber R. A., and Chhowalla M. Boron carbide: structure, properties, and stability under stress. Journal of the American Ceramic Society, Vol. 94, No. 11, pp. 3605-3628, 2011.

[12] Crouch I. G. Body armour-New materials, new systems. Defence Technology, Vol. 15, No. 3, pp. 241-253, 2019.

[13] Fejdyś M., Kośla K., Kucharska-Jastrząbek A., and Łandwijt M. Influence of ceramic properties on the ballistic performance of the hybrid ceramic-multi-layered UHMWPE composite armour. Journal of the Australian Ceramic Society, Vol. 57, pp. 149-161, 2021.

[14] Werhcit H., Kuhlmann U., Krach G., Higashi I., Lundström T., and Yu Y. Optical and electronic properties of the orthorhombic $MgAlB_{14}$-type borides. Journal of Alloys and Compounds, Vol. 202, No. 1-2, pp. 269-281, 1993.

[15] Cook B. A., Harringa J. L., Lewis T. L., and Russell A. M. A new class of ultra-hard materials based on $AlMgB_{14}$. Scripta materialia, Vol. 42, No. 6, pp. 597-602, 2000.

[16] Xie Z. L., DeLucca V., Haber R. A., Restrepo D. T., Todd J., Blair R. G., and Orlovskaya N. Aluminium magnesium boride: synthesis, sintering and microstructure. Advances in Applied Ceramics, Vol. 116, No. 6, pp. 341-347, 2017.

[17] Bodkin R. A synthesis and study of $AlMgB_{14}$. University of the Witwatersrand, 2005.

[18] Zhukov I. A., Nikitin P. Y., Vorozhtsov A. B., Perevislov S. N., Sokolov S. D., and Ziatdinov M. H. The use of intermetallic Al_xMg_y powder to obtain $AlMgB_{14}$-based materials. Materials Today Communications, Vol. 22, pp. 100848, 2020.

[19] Nikitin P. Y., Zhukov I. A., Boldin M. S., Perevislov S. N., and Chuvil'deev V. N. Spark plasma sintering, phase composition, and properties of $AlMgB_{14}$ ceramic materials. Russian Journal of Inorganic Chemistry, Vol. 66, pp. 1252-1256, 2021.

[20] Russell A. M., Cook B. A., Harringa J. L., and Lewis T. L. Coefficient of thermal expansion of $AlMgB_{14}$. Scripta Materialia, Vol. 46, No. 9, pp. 629-633, 2002.

[21] Tkachev D., Nikitin P., Zhukov I., Vorozhtsov A., Marchenko E., Verkhoshanskiy Y., and Belchikov I.

Structure and flexural strength of the hot-pressed $AlMgB_{14}$ ceramic. Physica Scripta, Vol. 98, No. 2, pp. 025703, 2023.

[22]Zhang Z, Xia F, Cao Z, and Yuan F. Experimental and Numerical Simulation Study of Dynamic Mechanical Behavior of $AlMgB_{14}$ Ceramic. International Conference on Mechanical System Dynamics. Pp. 1941-1953, 2023.

[23]Chen B. B. Study the failure characteristics of YAG under shock loading and the ballistic performance of transparent ceramic composite armor. Nanjing University of Science and Technology, 2020.

[24]Madhu V., Ramanjaneyulu K., Bhat T. B., and Gupta N. K. An experimental study of penetration resistance of ceramic armour subjected to projectile impact. International Journal of Impact Engineering, Vol. 32, No. 1-4, pp. 337-350, 2005.

[25]Gooch W. A., Burkins M. S., and Palicka R. Ballistic development of US high density tungsten carbide ceramics. 6th International Conference on Mechanical and Physical Behaviour of Materials under Dynamic Loading, Krakow, Poland, Vol. 10, No. PR9, pp. 741-746, 2000.

[26]Savio S. G., and Madhu V. Ballistic performance evaluation of ceramic tiles with respect to projectile velocity against hard steel projectile using DOP test. International Journal of Impact Engineering, Vol. 113, pp. 161-167, 2018.

[27]Liaw B. M., Kobayashi A. S., and Emery A. F. Theoretical model of impact damage in structural ceramics. Journal of the American Ceramic Society, Vol. 67, No. 8, pp. 544-548, 1984.

[28]Horsfall I., and Buckley D. The effect of through-thickness cracks on the ballistic performance of ceramic armour systems. International Journal of Impact Engineering, Vol. 18, No. 3, pp. 309-318, 1996.